



## Effect of calcination temperature on the structure of copper orthophosphates and their catalytic activity in the decomposition of 2-propanol

M. Ouchabi\*, M. Baalala, A. Elaissi, M. Bensitel\*

Laboratoire de Catalyse et Corrosion des Matériaux, Université ChouaibDoukkali, Faculté des Sciences d'El Jadida, BP. 20, El Jadida 24000, Morocco

Received 09 Feb 2016, Revised 07 Mar 2016, Accepted 13 Mar 2016

\*For correspondence: Email: [m.ouchabi@yahoo.fr](mailto:m.ouchabi@yahoo.fr); [mbensitel@yahoo.fr](mailto:mbensitel@yahoo.fr)

### Abstract

Libethenite  $\text{Cu}_2(\text{PO}_4)(\text{OH})$  was simply synthesized by heterogeneous reaction using a mixture of  $\text{Cu}(\text{NO}_3)_2 \cdot 6\text{H}_2\text{O}$ ,  $(\text{NH}_4)_2\text{HPO}_4$  and water at room temperature for 60 min. The thermogravimetric study indicates that the synthesized compound is stable below  $250^\circ\text{C}$  and its final decomposed product is  $\text{Cu}_3(\text{PO}_4)_2$ . The pure monoclinic phases of the synthesized  $\text{Cu}_2(\text{PO}_4)(\text{OH})$  and its final decomposed product  $\text{Cu}_3(\text{PO}_4)_2$  are verified by XRD technique. The presence of OH<sup>-</sup> ion and H<sub>2</sub>O molecule in the structure  $\text{Cu}_2(\text{PO}_4)(\text{OH})$  and the  $\text{PO}_4^{3-}$  ion into  $\text{Cu}_3(\text{PO}_4)_2$  structure are confirmed by FTIR technique. The decomposition test of isopropanol shows that the copper orthophosphate  $\text{Cu}_3(\text{PO}_4)_2$  catalysts have a strong propene selectivity, thus indicating the prevalence of acid sites. The thermal stability, the morphology based on Libethenite  $\text{Cu}_2(\text{PO}_4)(\text{OH})$  and acidity surface structure  $\text{Cu}_3(\text{PO}_4)_2$  of the studied compounds may affect their activities for potential applications in catalysis.

**Keywords:** Libethenite  $\text{Cu}_2(\text{PO}_4)(\text{OH})$ ; copper orthophosphate  $\text{Cu}_3(\text{PO}_4)_2$ , isopropanol conversion.

### 1. Introduction

The solid phase of inorganic phosphates constitutes a broad family of materials of considerable technological importance [1]. Orthophosphate salts of most elements of the periodic table are known and may include minerals, synthetic products, acid salts, hydrates and polymorphic varieties [2]. The continuing scientific interest in phosphate materials reflects their practical applications as fertilizers, catalysts, phosphors, ion conductors, piezoelectric materials, biotechnological materials and sorbents [3]. Copper-based compounds have been widely used in the area of catalysis, ion exchange, proton conductivity, intercalation chemistry, photochemistry, and chemistry materials [4,5]. For example, atacamite [ $\text{Cu}_2(\text{OH})_3\text{Cl}$ ], libethenite [ $\text{Cu}_2(\text{OH})\text{PO}_4$ ], lindgrenite [ $\text{Cu}_3(\text{OH})_2(\text{MoO}_4)_2$ ], and malachite [ $\text{Cu}_2(\text{OH})_2\text{CO}_3$ ] have been widely investigated due to their special crystal structures and applications [6-9]. Most of their properties are dependent on the composition, crystal type, shape, and size. The numerous investigations of the systems Cu-P-O and Cu-P-O-H have revealed their rich crystal chemistry. Copper can accommodate various coordinations from tetrahedral or square to pyramidal and octahedral. Thirteen different structures of copper phosphates or hydroxyphosphates have been discovered to date [10]. It is well accepted that there is a close relationship between the morphology and their properties of inorganic materials, that is, morphologies determine their properties since the crystal shape dictates the interfacial atomic arrangement of the material [11-16].

Acidic solids derived from metal orthophosphates are widely used to catalyze various reactions occurring at the gas/solid interface. Acid-base properties and redox properties are amongst important types of surface chemical properties of metal orthophosphate catalysts.

Decomposition of 2-propanol is frequently used as a test reaction to determine acid-base properties of different catalysts by many groups [17-23]. It has been reported that the decomposition of 2-propanol occurs by two parallel reactions: (i) the dehydration carried out in acid sites giving the propene and the isopropyl ether (DIPE) [24-25] and (ii) the dehydrogenation to acetone occurring on basic sites or both types of site (acid and basic) via a concerted mechanism. The aim of this paper is to study one of the methods of preparation leading to

Cu<sub>3</sub>(PO<sub>4</sub>)<sub>2</sub> solid, and to examine the treatment temperature effect on the transformation of precursor to active phase in the inert atmosphere and catalytic dehydration of isopropyl alcohol at 473–673 K temperature range.

## 2. Experimental

### 2.1. Solid Synthesis

Copper orthophosphates (CuP) was synthesized upon evaporation to dryness from aqueous solutions of Cu(NO<sub>3</sub>)<sub>2</sub>·3H<sub>2</sub>O and (NH<sub>4</sub>)<sub>2</sub>HPO<sub>4</sub>. The resulting solids were dried for 12 h at 120°C and were finally calcined in air at 250°C for 10 h, 450°C for 10 h and at 650°C for 10 h.



### 2.2. Characterization techniques

The X-ray diffraction (XRD) analysis was performed for the fresh catalyst using Bruker-eco D8 Advance diffract meter with Cu-K $\alpha$  radiation ( $\lambda = 1.5418 \text{ \AA}$ ). The XRD patterns were scanned from 5 to 70  $\theta$ .

TGA–DTA analysis has been recorded with a TA Instruments balance, model SDT 2966. It allows obtaining simultaneous DTA and TGA diagrams under similar experimental conditions. Experiments were performed under an N<sub>2</sub> flow, from 298 K to 1073 K using a heating rate of 5°C/min

Diffuse reflectance infrared spectra for the solids were recorded from 4000 to 400 cm<sup>-1</sup> on a Nicolet 460 spectrophotometer.

UV–Visible spectra in diffuse reflectance mode were recorded by Shimadzu UV-2400PC Series spectrometer, from 200 to 1000 nm.

The textural properties (i.e. specific area, pore volume) were determined by nitrogen adsorption at 77 K on a 3Flex Version 3.01 system.

### 2.3. Catalytic test

Decomposition of isopropanol was carried out in a fixed-bed type reactor with a continuous flow system at atmospheric pressure. The catalyst (50 mg, 200–500  $\mu\text{m}$  particle size) was placed in a reactor (Pyrex tube, 10 mm I.D) placed in a furnace. Before carrying out such catalytic activity measurements, each catalyst sample was activated by heating in a stream of nitrogen for 2 h at 673 K then cooled to the catalytic reaction temperature. The reactant, 2-propanol (3.7 kPa), was diluted in nitrogen by bubbling the gas through the liquid reactant in saturator maintained at 279 K, with contact time 5.76 h. The isopropanol decomposition was performed at a temperature between 433 and 673 K. Products were analyzed by on-line gas chromatography (Varian-3700 GC with a flame ionization detector FID) using a 10% 0 V–101 on Chromosorb-WHP (80/100 mesh) packed column (4m) maintained at 353 K. A blank test showed insignificant thermal reaction developed in the absence of the catalyst.

## 3. Results and discussion

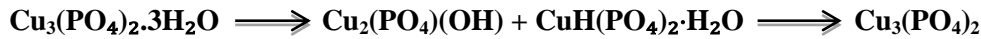
### 3.1. DTA and TG analyses

The TG/DTA curves of CuP samples are shown in Figure. 1. The TG curve of CuP shows three weight loss steps in the range of 50–670°C. The weight loss steps in the TG curve were observed in ranges of 50–150 and 150–320°C. The observed weight losses are 4.372 and 41.524% by weight, corresponding to 0.44 mole of water and 4.15 moles of ammonium nitrate and water. The first stage of the weight loss was related to the loss of moisture because it is not stable over 100°C. While the second stage was due to the loss of water molecules from overlapping reaction the loss of coordination water (dehydration reaction)[26-27]. These two stages appear in the corresponding DTA curve as two endothermic peaks (130 and 290°C).

The third stage of the weight loss can be attributed to the dehydroxylation of libethenite **Cu<sub>2</sub>(PO<sub>4</sub>)(OH)** which leads to an orthophosphate **Cu<sub>3</sub>(PO<sub>4</sub>)<sub>2</sub>**, corresponding to the endothermic peak located at 330°C.

The endothermic peak appeared at 605°C corresponds to the crystallization of Cu<sub>3</sub>(PO<sub>4</sub>)<sub>2</sub> orthophosphate.

The thermal decomposition of the studied  $\text{Cu}_2(\text{PO}_4)(\text{OH})$  involves the dehydration of the coordinated water molecule intramolecular and removal of OH groups. These processes finally could be presented as:



The final product of the thermal decomposition at  $T > 400^\circ\text{C}$  is found to be a copper orthophosphate  $\text{Cu}_3(\text{PO}_4)_2$ . For hydrate content analysis, the experimental total mass loss of 51.508 % is close to theoretical value calculated from the content of water and ammonium nitrate (3 mol  $\text{H}_2\text{O}$  and 2.15 mol ammonium nitrate). The formation of  $\text{Cu}_2(\text{PO}_4)(\text{OH})$  and its decomposed product  $\text{Cu}_3(\text{PO}_4)_2$  confirmed by XRD and FTIR analysis which is in agreement with this thermal analysis result.

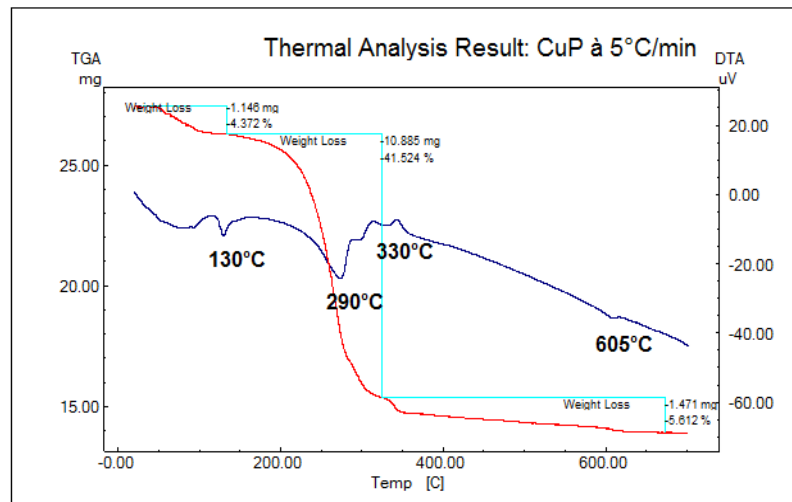


**Figure 1:** TGA-TDA curves for solid CuP

### 3.2. XRD analysis

Figure 2, Shows the evolution of the dried precipitated CuP solid calcined at different temperatures. The CuP solid treated at 523 K exhibits broad diffraction lines corresponding to libethenite  $\text{Cu}_2(\text{PO}_4)(\text{OH})$  (PDF Index Name : Copper Phosphate .ref cod: 01-083-1557), and  $\text{CuH}(\text{PO}_4)_2 \cdot \text{H}_2\text{O}$  (ref: cod: 00-012-0520). Beyond 723 K, a new crystalline material, corresponding to  $\text{Cu}_3(\text{PO}_4)_2$  added to  $\text{Cu}_2(\text{PO}_4)(\text{OH})$  could be clearly evidenced. Progressively with the increase in temperature, diffraction lines of the copper orthophosphate sharpen indicating a better crystallization of  $\text{Cu}_3(\text{PO}_4)_2$  (PDF Index Name :Copper Phosphate .ref cod: 01-070-0494). Parameters of the various copper phosphate crystalline phases are reported in Table 1.

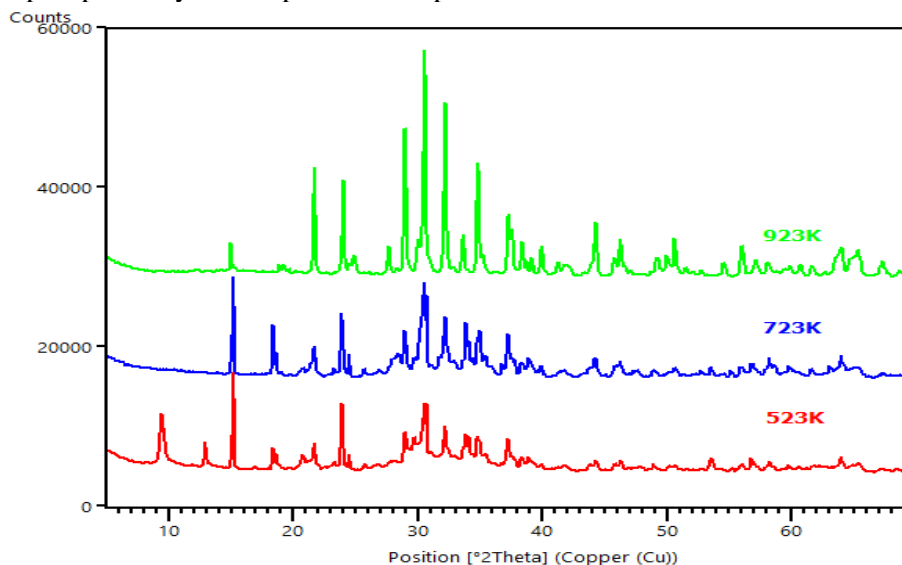


**Figure 2:** Evolution of XRD patterns with the temperature treatment.

**Table 1:** Average crystallite size and lattice parameter of  $\text{Cu}_2(\text{PO}_4)(\text{OH})$  and  $\text{Cu}_3(\text{PO}_4)_2$  calculated from XRD data.

Chemical formula	$\text{CuH}(\text{PO}_4)\cdot\text{H}_2\text{O}$	$\text{Cu}_2(\text{PO}_4)(\text{OH})$	$\text{Cu}_3(\text{PO}_4)_2$
Crystal system	monoclinic	Orthorhombic	Anorthic
Space group	P21/a	Pnnm	P-1
Space group number		58	2
a (Å):	a = 8.63	8.071	4.8550
b (Å):	b = 6.35	8.403	5.2880
c (Å):	c = 6.82	5.898	6.1840
$\alpha$ (°)		90.0000	72.3400
$\beta$ (°)	B = 94.14	90.0000	86.9900
$\gamma$ (°)		90.0000	68.5400

### 3.3. FTIR Spectroscopy

The FTIR spectra of the synthesized CuP (523K) powders (Fig. 3) assigned according to the literatures [33–35] reflect characteristic vibrations of  $\text{PO}_4^{3-}$  anion and  $\text{H}_2\text{O}$  molecules, respectively.

Vibrational bands of phosphate anion are observed in the regions of 1035-940, and 602- 546  $\text{cm}^{-1}$ . These bands are assigned to the  $\nu_{\text{as}}(\text{PO}_4^{3-})$ ,  $\nu_{\text{s}}(\text{PO}_4^{3-})$ , and  $\delta_{\text{s}}(\text{PO}_4^{3-})$  [28-29], respectively. The observed center bands at 1611  $\text{cm}^{-1}$  and 3227  $\text{cm}^{-1}$  are assigned to water bending  $\delta(\text{H}_2\text{O})$  and asymmetry stretching  $\nu_{\text{as}}(\text{O-H})$ ,  $\text{H}_2\text{O}$ , respectively implying the presence of crystalline hydrate. For characteristic vibration of CuP (973 K), FTIR bands are assigned according to the literature [30-31] based on the fundamental vibrating unit  $\text{PO}_4^{3-}$  anion. One of the most noteworthy features of the spectrum is the presence of the strong bands at 1120, 965-935, 608-527 and 406  $\text{cm}^{-1}$ . These bands can be assigned to the  $\nu_{\text{as}}(\text{PO}_4^{3-})$ ,  $\nu_{\text{s}}(\text{PO}_4^{3-})$ ,  $\delta_{\text{s}}(\text{PO}_4^{3-})$  and  $\delta_{\text{s}}(\text{POP})$ , respectively. In the various heat treatments, there is some changes in the spectra, firstly the progressive disappearance of the water vibration band, and secondly, the characteristic bands of groups  $(\text{PO}_4^{3-})$  refine, divide, which reflects a structural evolution of crystalline compound CuP. The structure of CuP evolves during the heat treatment which confirms the results XRD and TGA–DTA.

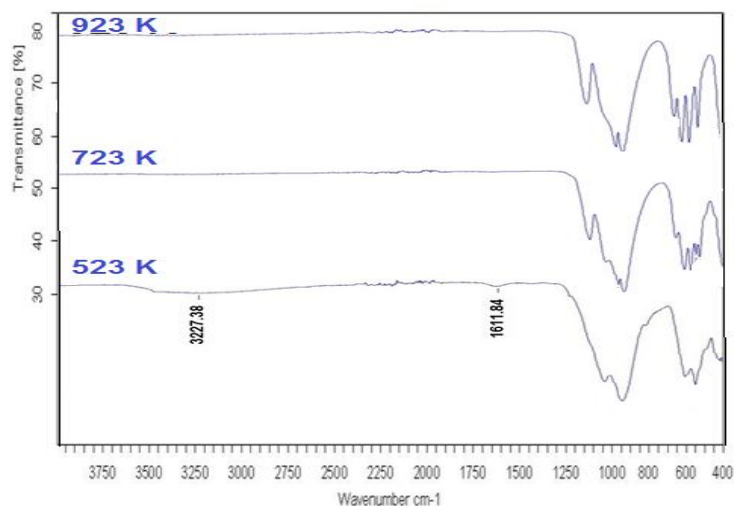
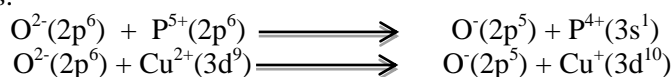


**Figure 3:** Evolution of IR spectra with the temperature treatment.

### 3.4. UV–Vis diffusive reflectance spectroscopic.

Diffuse-reflectance UV–VISIBLE spectra of the CuP samples calcined at different temperatures are compared in Figure 4. All spectra of CuP exhibit two major bands at 289 and 295 nm, were assigned to the charge-transfer transitions CTLM transitions between the ligand  $\text{O}^{2-}$  and isolated  $\text{Cu}^{2+}$  sites in octahedral coordination [32–34] and also be assigned to the CT transitions of P-O [35] or octahedrally coordinated  $\text{Cu}^{2+}$  centers in isolated states [36,37]. The increasing of treatment calcination for solids did not significantly change the positions of these two bands.



In addition, the CuP samples exhibit a small and broad visible absorption band with a maximum at 800 nm corresponding to d–d transitions ( $d^{10}-3d^94s^1$ ) of  $\text{Cu}^{2+}$ . This last  $\text{Cu}^{2+}$  is the only known ion having the  $3d^9$  configuration [38-42]. The energy diagram for  $d^9$  system in octahedral symmetry is just the inverse of that for octahedral  $d^1$  system. It is well known that the spectra of all solids containing copper ions have at least a wide and unsymmetrical broad visible band centered near 800 nm [40; 43]. A comparison with the spectra of aqueous and crystalline cupric complexes shows that the  $\text{Cu}^{2+}$  ions must be present in approximately octahedral coordination [41; 43; 44]. No appreciable changes of coordination of Cu(II) ion with temperature are detected from UV–vis–NIR spectra.

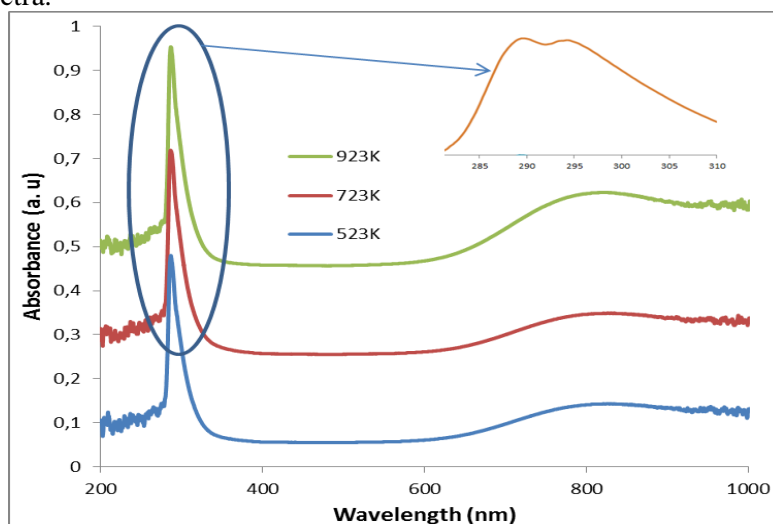


**Figure 4:** UV–Visible spectra of CuP samples calcined at 523 K, 723 K and 923 K.

### 3.5. Textural properties of the calcined solids

Figure 5 shows the  $\text{N}_2$  adsorption–desorption isotherms and Table 2 the specific surface area ( $S_{\text{BET}}$ ), total pore volume ( $V_p$  at  $P/P_0=0.98$ ), and average pore diameter for the synthesized solids calcined at 723 K. The profile of the adsorption isotherm of these solids is type II according to the IUPAC classification (International Union of Pure and Applied Chemistry). The hysteresis loop observed in these solids, as types H3, which are associated with materials possessing open-end cylindrical pores and exhibit no limiting adsorption at high  $P/P_0$  ratios that is observed with aggregates of plate-like particles giving rise to slit-shaped pores, respectively [45]. The average pore diameter for these solids is classed in the mesoporous range, according to Sing et al. [45].

However, an increasing of the temperature calcination in the samples decreases specific surface area and pore volume (Table 2), the same effect has been observed with the magnesium orthophosphates [46] that is probably due to the reduction of the porous volume concentration or to the pores replenishments.

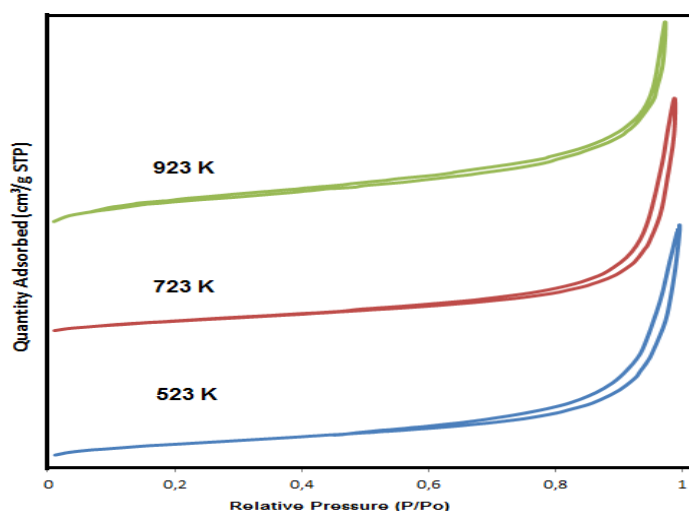


**Figure 5:**  $\text{N}_2$ -adsorption/desorption isotherm for CuP calcined at different temperature.

**Table 2:** Specific surface area ( $S_{BET}$ ), cumulative pore volume ( $V_p$ ) and average pore diameter ( $d_p$ ) for the synthesized solids.

Catalysts	$S_{BET}(m^2/g)$	$V_p (cm^3/g)$	$d_p(nm)$
CuP-523 K	4.1	0.011	10.3
CuP-723 K	6.1	0.017	11
CuP-923 K	3.2	0.006	6.5

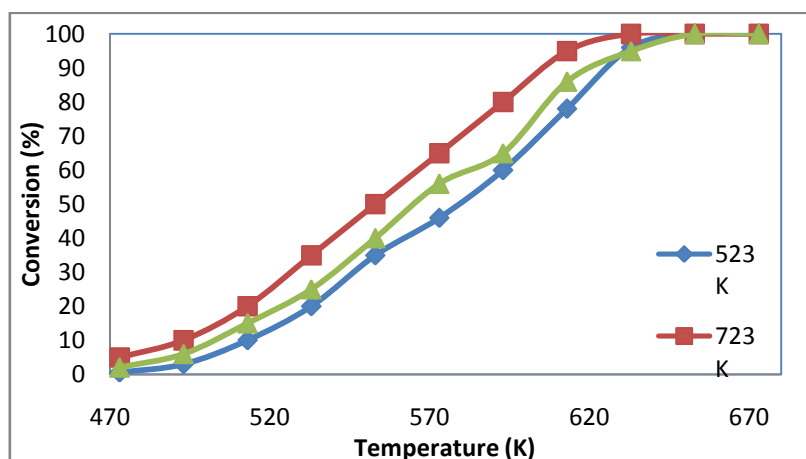
3.6. Catalytic activity

Table 3 shows the activity and selectivity in the isopropanol decomposition in the gas phase using the studied solids (CuP calcined at 523 K, 723 and 923 K). The main reactions promoted by these catalysts are dehydration of the 2-propanol to the corresponding alkenes (propene) and dehydrogenation to the carbonyl derivative (acetone). All values shown were obtained at  $t = 160$  min, shows that the activity remained constant over time.

**Table 3:** Isopropanol conversion (%) and selectivity towards propene, acetone at various temperatures over CuP catalyst calcined at 523, 723 and 923 K.

Temperature (K)	Catalysts								
	CuP calcined at 523 K			CuP calcined at 723 K			CuP calcined at 923 K		
	Conversion (%)	Selectivity (%)		Conversion (%)	Selectivity (%)		Conversion (%)	Selectivity (%)	
Propene		Acetone	Propene		Acetone	Propene		Acetone	
473	0.55	94	6	5	96	4	2	96	4
493	3	96	4	10	97	3	6	96	4
513	10	95	5	20	97	3	20	96	4
533	20	97	3	35	98	2	30	98	2
553	35	98	2	50	98	2	40	98	2
573	46	98	2	65	98	2	56	98	2
593	60	98	2	80	98	2	65	98	2
613	78	98	2	95	98	2	86	98	2
633	96	98	2	100	98	2	95	98	2
653	100	98	2	100	99	1	100	98	2
673	100	99	1	100	99	1	100	99	1

From Figure 6, the activity versus temperature trends for isopropanol decomposition of solids (CuP) correlate with the law of Langmuir. In addition, the activity increases with the increasing reaction temperature in all instances. The calcined solid at 723 K (CuP) exhibits catalytic activity higher than that calcined at 923 K (CuP) and that calcined at 523K at a reaction temperature of 473 K, and similar results obtained at a reaction temperature of 493 K, and similar results obtained at a reaction temperature  $> 633$  K.



**Figure 6:** Isopropanol decomposition as function of the reaction temperature on CuP catalysts surface.

The decrease of the catalytic activity versus the calcination temperature is probably due to the dehydration of the catalyst surface.

The latter catalyst (CuP) exhibits high selectivity to propene in all reaction temperatures. This higher selectivity is attributed to the increase of active site numbers on the surface of catalysts. It can be also correlated to the acidity of the catalyst [47, 48]. This selectivity attains 99% in all reaction temperature 573 K (Table 3). In other words, the solid contains CuP phase favored dehydration over dehydrogenation, therefore the solid can be assumed to be essentially acid.

In perspective, this copper orthophosphate will be used as a support for active phase such as vanadium oxide and NiMo.

## Conclusions

The results obtained in this work show that the synthesis of copper phosphate depends on the procedure of preparation. The thermal treatment at high temperature under inert atmosphere leads to copper orthophosphate (CuP) whereas the treatment below 673 K leads to libethenite, as shown by XRD analysis and confirmed by DTA–TGA results. The results obtained from FT-IR and UV–Vis spectroscopy are in agreement with the previous results, showing that this technique is efficient for the analysis of copper–phosphate materials. The synthetic catalysts showed high activity and selectivity towards propene for the isopropanol decomposition at low reaction temperature in comparison with the others catalysts. It was found that the CuP (723 K) samples exhibited high catalytic activity in the 2-propanol decomposition than CuP (923K) samples. The 2-propanol dehydration to propene is the predominant reaction and proceeds via an elimination E1-like mechanism catalyzed by acid sites.

The results obtained are necessary for theoretical study, applications development, and industrial production of metal phosphates, which may have interesting and potential applications for further works.

## References

1. Finn R.C., Zubietta J., Haushalter R.C., *Prog. Inorg. Chem.* 51 (2002) 451.
2. Corbridge D.E.C., Phosphorus, Elsevier, Amsterdam, ISBN ; 10: 0444424687, (1978).
3. Kanazawa T., Inorganic phosphate materials, in: *Materials Science Monographs*, vol. 52, Elsevier, Amsterdam, 1989.
4. Rodriguez-Clemente R., Serna C.J., Ocana M., Matijevic E.J., *J. Cryst. Growth* 143(1994) 277–286.
5. Wen X., Xie Y., Choi C.L., Wang K.C., Li X., Yang Y.S., *Langmuir* 21 (2005)4729–4737.
6. Lichenegger H.C., Schoberl T., Bartl M.H., Waite H., Stucky G.D., *Science* 298 (2002) 389–392.
7. Frost R.L., Klopogge T., Williams P.A., Martens W., Johnson T.E., Leverett P., *Spectrochim. Acta A* 58 (2002) 2861–2868.
8. Xiao F., Sun J., Meng X., Yu R., Yuan H., Jiang D., Qiu S., Xu R., *Appl. Catal. A-Gen.*207 (2001) 267–271.
9. Palache C., *Am. Miner.*, 20 (1935) 484–491.
10. Baies R., Caignaert V., Pralong V., Raveau B., *Inorg.Chem.* 44 (2005) 2376–2380.
11. Chen S., Yu S., Jiang J., Li F., Liu Y., *Chem. Mater.* 18 (2006) 115–122.
12. Pan C., Gu Z., Dong L., *Acta Chim. Sinica* 17 (2009) 1981–1986.
13. Akla A., Howari H., *J. Phys. Chem. Solids* 70 (2009) 1337–1343.
14. Khalavka Y., Sonnichsen C., *Adv. Mater.* 20 (2008) 588–591.
15. Xu J., Xue D., *J. Phys. Chem. Solids* 67 (2006) 1427–1431.
16. Huang X., Guo C., Zuo J., Zheng N., Stucky G.D., *Small* 5 (2009) 361–365.
17. Aramendi´a M.A., Borau V., Jime´nez C., Marinas J.M., Porras A., Urbano F.J., *J. Catal.* 161 (1996) 829.
18. Benes L., Galli P., Massucci M.A., Melanoma K., Patrono P., Zima V., *J. Therm. Anal.* 50 (1997) 355.
19. El-Molla S.A., Hammed M.N., El-Shobaky G.A., *Mater. Lett.*58 (2004) 1003.
20. El-Shobaky H.G., Ahmed A.S., Radwan N.R.E., *J. Colloid Surf. A: Physicochem. Eng. Aspects* 274 (2006) 138.
21. Lopez T., Manriquez M.E., Gomez R., Campero A., Llanos M.E., *Mater. Lett.* 46 (2000) 21.

22. Ortiz-Islasa E., Lopez T., Navarrete J., Bokhimi X., Gomez R., *J. Mol. Catal. A: Chem.* 228 (2005) 345.
23. Oukerroum J., Badrou L., Bensitel M., Sadel A., Zahir M., *Ann. Chim. Sci. Mater.* 26 (2001) 529.
24. Sadiq M., Sahibed-dine A., Baalala M., Bensitel M., Payen E., Lamonier C., Leglise J., *Phys. Chem. News* 37 (2007)107.
25. Satoh N., Hayashi J.I., Hattori H., *Appl. Catal. A: Gen.* (2000) 202- 207.
26. Sadiq M., Bensitel M., Lamonier C., Leglise L., *Solid State Sciences* 10 (2008) 434-437.
27. Banjong Boonchom., NaratipVittayakorn., *Ceramics International*, 38 (2012) 411–415
28. Onmura N., Tagawa T., Goto S., *Appl. Catal A: Gen* 166 (1998) 321
29. AbadzhievaP., Tzokov I., Uzunow V., MinkovD., Klissurski V., Rives, *React.*
30. Colthup N.B., Daly L.H., Wiberley S.E., *Introduction to Infrared and Raman Spectroscopy*, Academic Press, New York, 1964.
31. Steger E., Kaßner B., *Die infrarotspektren von wasser freischwer metall-Diphosphaten*, *Spectrochimica Acta*, 24A (1968) 447–456.
32. Lehmann G. Z., *Phys. Chem. Neue Folge* 72 (1970) 279–297.
33. Bordiga S., Buzzoni R., Geobaldo F., Lamberti C., Giamello E., Zecchina A., Leofanti G., Petrini G., Tozzola G., Vlaic G., *J. Catal.* 158 (1996) 486–501.
34. Tippins H.H., *Phys. Rev. B* 1 (1970) 126–135.
35. Yuan Q., Zhang Q., Wang Y., *J. Catal.* 233 (2005) 221–233.
36. Yashnik S.A., Ismagilov Z.R., Anufrienko V.F., *Catal. Today* 110 (2005) 310–322.
37. Kubacka A., Wang Zh., Sulikowski B., Corberan V.C., *J. Catal.* 250 (2007) 184–189.
38. Cotton F.A., Wilkinson G., Murrillo C.A., Bochmann M., *Advanced Inorganic Chemistry*, 6th ed., John-Wiley-Interscience, New York, 1999.
39. Bates T., in: J.D. Mackenzie (Ed.), *Modern Aspects of the Vitreous State*, Butter worths, London., vol.2 (1962) 195.
40. Bamford C.R., *Color Generation and Control in Glass*, Elsevier Science Publisher, Amsterdam, 1977.
41. Jorgensen C.K., *Acta Chem. Scand.* 11 (1957) 73.
42. Duran A., Fernandez Navarro J.M., *Phys. Chem. Glasses* 26 (1985) 126.
43. Cable M., Xiang Z.D., *Phys. Chem. Glasses* 30 (1989) 237.
44. Morsi M.M., Metwalli E.S., Mohamed A.A., *Phys. Chem. Glasses* 40 (1999) 314.
45. Sing, K.S.W., Everest, D.H.R., Haul, R.A.W., Moscou, L., Pierotti, R.A., Rouque´rol, J., Siemieniewska, T., *Pure Appl. Chem.* 57 (1985) 603.
46. Sadiq M., Sahibed-dine A., Baalala M., Nohair K., Abdennouri M., Bensitel M., Lamonier C., Leglise J., *Arabian Journal of Chemistry* 4 (2011) 449–457
47. Zhu, Y.J., Li, J., Xie, X.F., Yang, X.G., Wu, Y., *J. Mol. Catal. A: Chem.* 246 (2006) 185.
48. Elassal Z., Groula L., Nohair K., Sahibed-dine A., Brahmi R., Loghmarti M., Mzerd A., Bensitel M., *Arabian Journal of Chemistry* 4 (2011) 313–319

(2016); <http://www.jmaterenviromsci.com/>